Two Neuronal Nicotinic Acetylcholine Receptors, α4β4 and α7, Show Differential Agonist Binding Modes*□S

Nyssa L. Puskar[‡], Xinan Xiu[‡], Henry A. Lester[§], and Dennis A. Dougherty[‡1]

From the Divisions of [‡]Chemistry and Chemical Engineering and [§]Biology, California Institute of Technology, Pasadena, California 91125

Nicotinic acetylcholine receptors (nAChRs) are pentameric, neurotransmitter-gated ion channels responsible for rapid excitatory neurotransmission in the central and peripheral nervous systems, resulting in skeletal muscle tone and various cognitive effects in the brain. These complex proteins are activated by the endogenous neurotransmitter ACh as well as by nicotine and structurally related agonists. Activation and modulation of nAChRs has been implicated in the pathology of multiple neurological disorders, and as such, these proteins are established therapeutic targets. Here we use unnatural amino acid mutagenesis to examine the ligand binding mechanisms of two homologous neuronal nAChRs: the α4β4 and α7 receptors. Despite sequence identity among the residues that form the core of the agonist-binding site, we find that the α4β4 and α7 nAChRs employ different agonist-receptor binding interactions in this region. The α4β4 receptor utilizes a strong cation-π interaction to a conserved tryptophan (TrpB) of the receptor for both ACh and nicotine, and nicotine participates in a strong hydrogen bond with a backbone carbonyl contributed by TrpB. Interestingly, we find that the α7 receptor also employs a cation-π interaction for ligand recognition, but the site has moved to a different aromatic amino acid of the agonist-binding site depending on the agonist. ACh participates in a cation-π interaction with TyrA, whereas epibatidine participates in a cation-π interaction with TyrC2.

Nicotinic acetylcholine receptors (nAChRs)[2] belong to the Cys loop superfamily of neurotransmitter-gated ion channels, which also includes $GABA_A$ and $GABA_C$, glycine, and serotonin type 3 (5-HT$_3$) receptors. These transmembrane proteins are essential for proper rapid synaptic transmission in the central and peripheral nervous systems (1). One or more nAChRs are implicated in pathophysiology and/or therapy of multiple neurological and psychiatric disorders including addiction, schizophrenia, Parkinson disease, Alzheimer disease, pain, attention deficit hyperactivity disorder, epilepsy, depression, and congenital myasthenic syndromes (2, 3).

The nAChR is the longest known, most studied neuroreceptor. Early work established a nicotinic pharmacophore comprised of a cationic N and a hydrogen bond-accepting group separated by an appropriate distance (4, 5). This pharmacophore is also present in the potent agonist epibatidine and in cytisine, which has served as an important lead compound for discovery of new nicotinic drugs (6). Although the overall layout of the receptor has been delineated by cryo-electron microscopy images of the *Torpedo californica* nAChR (7), the present work focuses on the agonist-binding site. Ligands bind at a subunit interface in the large, N-terminal, extracellular domain. A major advance in the field was the discovery and structural characterization of the family of snail acetylcholine-binding proteins, which share 20–25% sequence identity with the extracellular domain of the nAChR (8, 9). The cationic moiety of ACh interacts with a cluster of aromatic amino acids. These aromatic residues were first identified by photoaffinity labeling and mutagenesis experiments of the full receptor and subsequently located by the acetylcholine-binding protein crystal structures (1, 8). The binding site "aromatic box" is formed by five residues: four contributed by the "principal" subunit (TyrA, TrpB, TyrC1, and TyrC2) and one contributed from the "complementary" surface or subunit (TrpD), and these five aromatics are completely conserved within the nAChR family (Fig. 1). The hydrogen bond acceptor of the agonist interacts with residues from the complementary subunits (β in neuronal nAChRs and γ, δ, and ε in the muscle-type nAChR) (10).

To date, 16 mammalian genes have been identified that encode nAChR subunits, termed α1–α7, α9, α10, β1–β4, δ, γ, and ε. The muscle-type nAChR, post-synaptically located at the neuromuscular junction, has a uniquely precise stoichiometry of (α1)$_2$β1γδ (fetal form; the adult form is (α1)$_2$β1δε). Most other nAChRs are located post- or pre-synaptically in autonomic ganglia and cholinergic neurons throughout the central nervous system; some of the so-called "neuronal" nAChRs, such as the α7 subtype studied in this paper, also occur on non-neuronal cells (2,11). Neuronal nAChRs have variable stoichiometries formed from various combinations of α and β subunits (11). This large collection of closely related receptors— current estimates are that as many as 25 nAChR subtypes are active in humans—presents special challenges to drug discovery efforts (3). It seems certain that therapeutics directed toward specific neurological disorders will require selectivity in terms of which nAChR subtype(s) is targeted.

In previous work, we have studied the muscle-type and neuronal α4β2 receptors (12–15). Here we extend our studies of the principal component of the agonist-binding site to two

---

□S The on-line version of this article (available at http://www.jbc.org) contains supplemental Tables S1–S3.
[1] To whom correspondence should be addressed: Division of Chemistry and Chemical Engineering, California Institute of Technology, 1200 E California Blvd., Pasadena, CA 91125. Tel.: 626-395-6089; Fax: 626-564-9297; E-mail: dadougherty@caltech.edu.
[2] The abbreviations used are: nAChR, nicotinic acetylcholine receptor; 5-CN-Trp, 5-cyano-tryptophan; 4-MeO-Phe, 4-methoxy-phenylalanine.
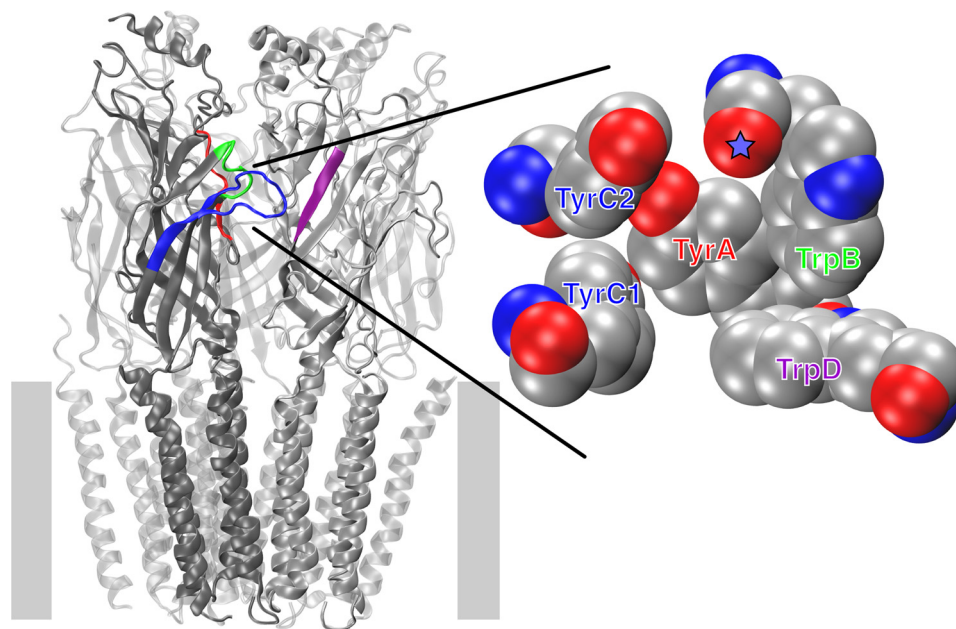
FIGURE 1. **nAChR structure.** *Left panel*, global layout of the nAChR based on cryo-electron microscopy of the Torpedo receptor (Protein Data Bank code 2BG9) (7). The position of the membrane is denoted by *gray bars*. A large intracellular domain that is only partly observed in the structure is omitted. *Right panel*, enlargement of agonist-binding site from acetylcholine-binding protein (Protein Data Bank code 1I9B) (8). Aromatic residues forming the ligand-binding site are indicated. Note that TyrA, TrpB, TyrC1, and TyrC2 are contributed by the α subunit, whereas TrpD is contributed by the non-α subunit. Coloring of the residue labels matches that of the corresponding loops in the full structure. Backbone carbonyl contributed by TrpB is denoted by a *star*.

other subtypes of the nAChR family, the neuronal α4β4 and α7 receptors. The α4 and β4 subunits colocalize in brain regions implicated in behavioral responses to nicotine, such as the medial habenula (2, 16). The β4 subunit is more commonly expressed with the α3 subunit, where it forms the major nAChR of autonomic ganglia, and a cluster of genes including the β4, α3, and α5 subunits are repeatedly identified in genome wide association studies and candidate gene studies that focus on nicotine dependence (2, 17). It is not yet known whether these associations arise from peripheral or central nervous system nAChRs. Further supporting the role of the β4 subunit in acute responses to nicotine, $β4^{-/-}$ knock-out mice are more resistant to nicotine-induced seizures when compared with wild type mice (2). The pharmacology of the α4β4 nAChR differs markedly from that of the muscle-type and α4β2 receptors, providing a valuable comparison for the structure-function studies employed here.

The homopentameric α7 nAChR is one of the most prevalent neuronal nAChR subtypes and is a potential therapeutic target in schizophrenia, Alzheimer disease, and inflammation (18–20). These receptors are richly expressed in most forebrain, midbrain, and hindbrain regions, as well as in some non-neuronal cells (2, 21). Brain expression is heaviest in the neonatal period, when the endogenous ligand may be choline; even in adults, most neurons exhibit ACh responses with characteristic α7 waveforms and pharmacology (22–24). In neurons and heterologous expression systems, α7 nAChRs exhibit responses that desensitize within 10–100 ms (25), but even the peak α7 responses are less sensitive to agonists than are α4β2 or α4β4 responses (2, 26). Despite the widespread expression of the α7 nAChR, homozygous α7 knock-out mice are viable (27). Mouse strains with low expression of α7 nAChRs provide a useful model for schizophrenia (28, 29), and α7 nAChRs may be acti-

vated by the high concentrations of nicotine that are produced by the heavy smoking habits of many schizophrenics (30, 31).

Here we use unnatural amino acid mutagenesis to investigate the ligand binding modes of the neuronal α4β4 and α7 nAChRs (Fig. 2). In the α4β4 receptor, we establish a strong cation-π interaction to a conserved tryptophan (TrpB) of the receptor for both ACh and nicotine. Nicotine also participates in a strong hydrogen bond with the backbone carbonyl contributed by TrpB. Overall, the binding patterns are similar to that reported for the α4β2 receptor (15). The α7 receptor also employs a cation-π interaction for ligand recognition, but surprisingly, we find that the locus has moved to a different aromatic amino acid of the agonist-binding site depending on the agonist. ACh participates in a cation-π interaction with TyrA, whereas the nicotine analog epibatidine participates in a cation-π interaction with TyrC2.

EXPERIMENTAL PROCEDURES

Molecular Biology—nAChR subunits of human α4 and β4 were in pGEMhe, whereas rat α7 was in pAMV. Site-directed mutagenesis was performed using the QuikChange protocol (Stratagene). For nonsense suppression experiments, the site of interest within the nAChR subunit was mutated to an amber stop codon. Circular DNA for α4 and β4 was linearized with NheI. Circular α7 DNA was linearized with NotI. After purification (Qiagen), linearized DNA was used as a template for runoff *in vitro* transcription using T7 mMessage mMachine kit (Ambion). hRIC-3 cDNA in pGEM was obtained from Dr. Miller Treinin at Hebrew University. Circular hRIC-3 DNA was linearized with XhoI, and mRNA was prepared as previously described.

THG73 (32) was used as the amber suppressor tRNA. The nitroveratryloxycarbonyl-protected cyanomethyl ester form of
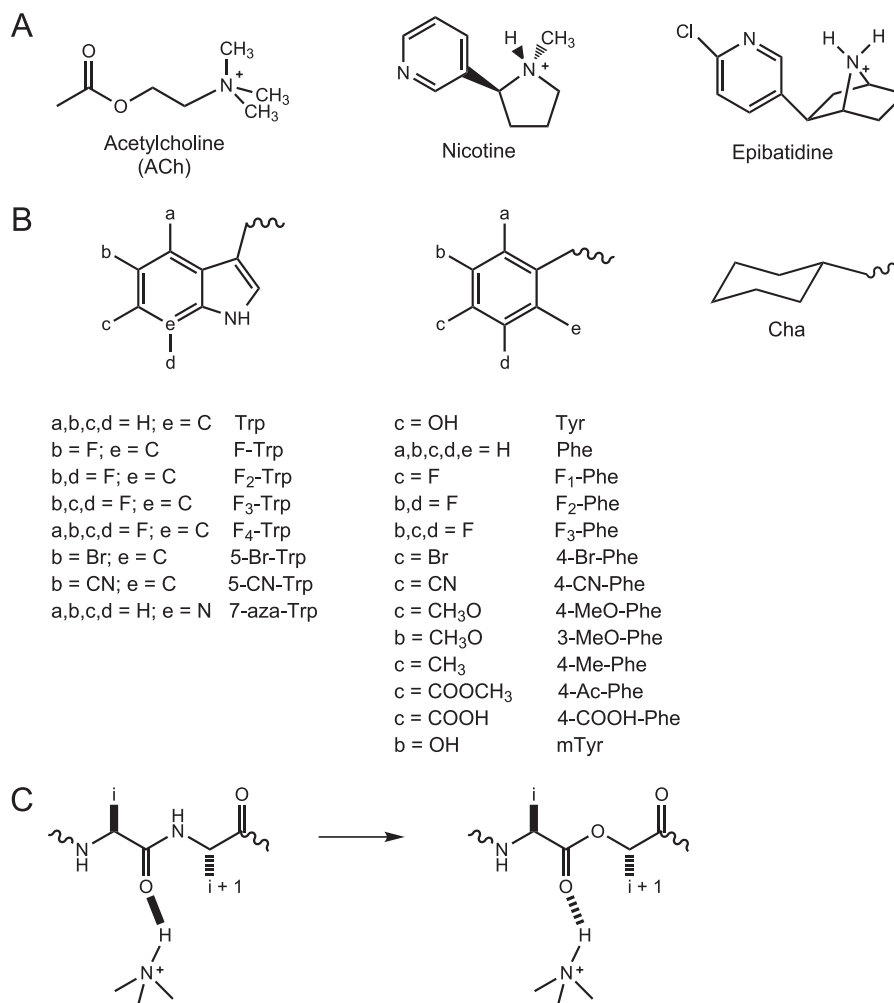
FIGURE 2. **Key structures employed in this study.** *A*, structures of ACh, nicotine, and epibatidine. *B*, unnatural amino acids used in the present study. If not indicated, a, b, c, or d group is H. *C*, α-hydroxy acid incorporation; the backbone ester strategy for modulating a hydrogen bond. *F-Trp*, 5-fluoro-tryptophan; *F₂-Trp*, 5,7-difluoro-tryptophan; *F₃-Trp*, 5,6,7-trifluoro-tryptophan; *F₄-Trp*, 4,5,6,7-tetrafluoro-tryptophan; *5-Br-Trp*, 5-bromo-tryptophan; *7-aza-Trp*, 7-aza-tryptophan; *F₁-Phe*, 4-flouro-phenylalanine; *F₂-Phe*, 3,5-diflouro-phenylalanine; *F₃-Phe*, 3,4,5-triflouro-phenylalanine; *4-Br-Phe*, 4-bromo-phenylalanine; *4-CN-Phe*, 4-cyano-phenylalanine; *3-MeO-Phe*, 3-methoxy-phenylalanine; *4-Me-Phe*, 4-methyl-phenylalanine; *4-Ac-Phe*, 4-acetyl-phenylalanine; *4-COOH-Phe*, 4-carboxy-phenylalanine; *mTyr*, *meta*-tyrosine.

unnatural amino acids and α-hydroxythreonine cyanomethyl ester were synthesized, coupled to dinucleotide dCA, and enzymatically ligated to 74-nucleotide THG73 tRNA$_{CUA}$ as previously reported (33). Crude tRNA amino acid product was used without desalting, and the product was confirmed by MALDI-TOF MS on 3-hydropicolinic acid matrix. Deprotection of the nitroveratryloxycarbonyl group on the tRNA-amino acid was carried out by photolysis for 5 min prior to co-injection with mRNA containing the UAG mutation at the site of interest.

Microinjection—Stage V–VI *Xenopus laevis* oocytes were employed. Co-injection of α4:β4 mRNA at a ratio of 1:1 by mass or lower yielded wild type $(α4)_2(β4)_3$ receptors, whereas a ratio of 30:1 by mass or higher produced pure populations of $(α4)_3(β4)_2$. If an unnatural amino acid was to be incorporated into the α4 subunit to produce a $(α4)_2(β4)_3$ receptor, then a mass ratio of 2:1 for α4:β4 mRNA was injected into each oocyte. For α4β4 experiments, the total mRNA injected was 25–65 ng/oocyte depending on the relative expression level. For α7 T6′S experiments, 10–25 ng of α7 T6′S mRNA was co-injected with 20 ng of hRIC-3 mRNA per oocyte. For all of the suppression experiments, ~15 ng of tRNA/cell was used. Each oocyte was injected with 50 nl of RNA solution, and the oocytes were incubated for 24–48 h at 18 C in culture medium (ND96$^+$ with 2.5% horse serum). In the case of low expressing mutant receptors, a second injection was required 24 h after the first injection. As a negative control for all suppression experiments, 76-nucleotide tRNA (dCA ligated to 74-nucleotide tRNA) was co-injected with mRNA in the same manner as fully charged tRNA.

Electrophysiology—Acetylcholine chloride and (−)-nicotine tartrate were purchased from Sigma/Aldrich/RBI, and drug dilutions were prepared from 1 M *aq* stock solutions. (±)-Epibatidine was purchased from Tocris, and drug dilutions were prepared from a 50 mM stock solution (1:1 H₂O:EtOH). For α4β4 experiments, drug dilutions were prepared in calcium-free ND96 buffer. For α7 T6′S experiments, drug dilutions were prepared in calcium-containing ND96 buffer.

Ion channel function was assayed using the OpusXpress 6000A (Molecular Devices Axon Instruments) in two-electrode voltage clamp mode. The oocytes were clamped at a holding

potential of -60 mV. For $\alpha4\beta4$ receptors, 1 ml of each drug solution was applied to the clamped oocytes for 12 s and followed by a 2-min wash with calcium-free ND96 buffer between each concentration. For $\alpha7$ T6′S receptors, 1 ml of each drug solution was applied for 30 or 12 s, followed by a 5-min wash step with calcium-containing ND96 buffer between each concentration. The data were sampled at 125 Hz and filtered at 50 Hz.

Data Analysis—Dose-response data were obtained for at least six concentrations of agonists and for a minimum of five oocytes (from two different batches). Mutants with I_{max} of at least 100 nA of current were defined as functional. The EC_{50} and Hill coefficient (n_H) values were calculated by fitting the averaged, normalized dose-response relation to the Hill equation. All of the data are reported as the means $\pm$ S.E.

RESULTS

Challenges in Studying Neuronal nAChRs with Unnatural Amino Acids—The nonsense suppression methodology for incorporating unnatural amino acids into receptors and ion channels expressed in *Xenopus* oocytes has proven to be broadly applicable, including studies of serotonin ($5\text{-}HT_3$) receptors, GABA receptors, glycine receptors, K^+ and Na^+ channels, and G protein-coupled receptors such as the D2 dopamine and M2 muscarinic ACh receptors (13, 33–37). Studies of the muscle-type nAChR have long been straightforward, but attempts to apply the methodology to neuronal nAChRs were initially frustrated by several factors. These issues include poor expression in *Xenopus* oocytes and some intrinsic pharmacological properties of the receptors. Here, we report the strategies used to overcome these obstacles in both the $\alpha4\beta4$ and $\alpha7$ receptors.

First, expression of the nAChRs in *Xenopus* oocytes yields variable stoichiometries. This can be problematic, because interpretation of subtle structure-function studies requires a homogeneous collection of receptors. Several studies of other receptor subtypes have shown that biasing the ratios of subunit mRNAs injected into the oocyte can influence subunit stoichiometry (15, 38), and we have found similar results in our previous studies of unnatural amino acids in the $\alpha4\beta2$ receptor (15). For the $\alpha4\beta2$ nAChR, the $(\alpha4)_2(\beta2)_3$ form is the higher sensitivity form for nicotine, and chronic exposure to nicotine leads to up-regulation of this form at the expense of $(\alpha4)_3(\beta2)_2$ in a variety of cell types (38, 39).

In initial studies of the $\alpha4\beta4$ receptor, we observed variable dose-response curves and anomalously low Hill coefficients, indicating a mixed population of receptors. By biasing the subunit mRNA ratios, we observed two dominant $\alpha4\beta4$ receptor populations, which we have assigned as $(\alpha4)_2(\beta4)_3$ and $(\alpha4)_3(\beta4)_2$. To facilitate comparisons and to emphasize the critical role of the β subunit in defining drug selectivity at nAChRs, our studies of the $\alpha4\beta4$ nAChR have focused on the $(\alpha4)_2(\beta4)_3$ form. We found that injection of an mRNA ratio $\alpha4{:}\beta4$ of 1:1 or lower produces a pure population of $(\alpha4)_2(\beta4)_3$, whereas a ratio of 30:1 or higher is necessary to produce pure populations of $(\alpha4)_3(\beta4)_2$ (supplemental Table S1).

Studies of the homopentameric $\alpha7$ nAChR also presented several challenges, including poor expression and agonist con-

TABLE 1

EC_{50} values (μM) for mutant $(\alpha4)_2(\beta4)_3$ and $\alpha7$ nAChRs

The EC_{50} values are $\pm$ S.E. NR, no response; ND, not determined; F_1-Trp, 5-fluoro-tryptophan; F_2-Trp, 5,7-difluoro-tryptophan; F_3-Trp, 5,6,7-trifluoro-tryptophan; F_4-Trp, 4,5,6,7-tetrafluoro-tryptophan; 5-Br-Trp, 5-bromo-tryptophan; 7-aza-Trp, 7-aza-tryptophan; F_1-Phe, 4-flouro-phenylalanine; F_2-Phe, 3,5-difluoro-phenylalanine; F_3-Phe, 3,4,5-triflouro-phenylalanine; 4-Br-Phe, 4-bromo-phenylalanine; 4-CN-Phe, 4-cyano-phenylalanine; 3-MeO-Phe, 3-methoxy-phenylalanine; 4-Me-Phe, 4-methyl-phenylalanine; 4-Ac-Phe, 4-acetyl-phenylalanine; 4-COOH-Phe, 4-carboxy-phenylalanine; Cha, cyclohexylalanine; Tah, threonine-α-hydroxy.

| | $\alpha4\beta4$ | | $\alpha7$ | |
	ACh	Nicotine	ACh	Epibatidine
Wild type	13 ± 1	2.4 ± 0.1	94 ± 3	0.34 ± 0.01
TyrA				
Tyr	17 ± 1	3.1 ± 0.2	93 ± 10	0.38 ± 0.05
Phe	260 ± 11	11 ± 0.4	4500 ± 200	3.0 ± 0.04
F_1-Phe	254 ± 21	6.6 ± 0.6	1400 ± 100	3.0 ± 0.1
F_2-Phe	159 ± 16	7.1 ± 0.4	4100 ± 200	18 ± 1
F_3-Phe	158 ± 14	7.7 ± 0.5	6000 ± 200	15 ± 2
4-Br-Phe	49 ± 1	3.5 ± 0.2	78 ± 3	0.34 ± 0.04
4-CN-Phe	855 ± 63	80 ± 6	1700 ± 100	1.8 ± 0.2
4-MeO-Phe	50 ± 2	4.2 ± 0.2	103 ± 3	0.94 ± 0.09
TrpB				
Trp	15 ± 1	2.0 ± 0.1	93 ± 9	0.38 ± 0.02
F_1-Trp	41 ± 2	5.6 ± 0.5	ND	ND
F_2-Trp	51 ± 2	8.1 ± 0.9	87 ± 5	0.62 ± 0.04
F_3-Trp	NR	73 ± 6	ND	ND
F_4-Trp	NR	190 ± 116	ND	ND
5-Br-Trp	28 ± 1	7.1 ± 0.5	ND	ND
5-CN-Trp	254 ± 27	46 ± 3	63 ± 4	0.14 ± 0.03
7-aza-Trp	162 ± 17	28 ± 2	ND	ND
TyrC1				
Tyr	11 ± 1	1.8 ± 0.1	98 ± 5	ND
Phe	1100 ± 126	60 ± 2	8600 ± 600	ND
4-Br-Phe	1400 ± 140	65 ± 9	ND	ND
4-CN-Phe	2700 ± 500	156 ± 13	ND	ND
4-MeO-Phe	550 ± 37	75 ± 9	NR	ND
TyrC2				
Tyr	11 ± 1	2.2 ± 0.1	94 ± 2	0.35 ± 0.04
Phe	26 ± 1	2.0 ± 0.2	560 ± 20	3.8 ± 0.4
F_1-Phe	ND	ND	86 ± 5	1.1 ± 0.02
F_2-Phe	ND	ND	870 ± 40	13 ± 1
F_3-Phe	ND	ND	1300 ± 100	16 ± 1
4-Br-Phe	4.5 ± 0.3	0.36 ± 0.01	51 ± 2	0.32 ± 0.02
4-CN-Phe	11 ± 1	2.5 ± 0.1	150 ± 10	2.1 ± 0.04
4-MeO-Phe	13 ± 1	1.3 ± 0.1	160 ± 10	0.41 ± 0.01
Trp(B+1)				
Thr	15 ± 1	1.7 ± 0.1	47 ± 2	0.45 ± 0.01
Tah	12 ± 1	23 ± 1	11 ± 1	0.95 ± 0.03

centration-dependent desensitization; the latter impedes accurate measurement of dose-response relations. To overcome the issue of poor expression, we co-expressed the $\alpha7$ nAChR with the human homolog of the RIC-3 protein (hRIC-3). Other studies have shown that co-expression with hRIC-3 enhances surface expression of $\alpha7$ nAChRs, presumably by aiding the folding, assembly, and/or trafficking of the $\alpha7$ protein (40–44). Regarding desensitization, we introduced a mutation into the M2 transmembrane helix, termed T6′S. Previous work established that this mutation, which lies ~60 Å from the agonist-binding site, decreases desensitization without disrupting other aspects of receptor pharmacology (45). All of the studies of the $\alpha7$ receptor reported here include this mutation.

Nicotine is not a potent agonist for $\alpha7$ receptors; this complicates analyses of mutant receptors with elevated EC_{50} values. On the other hand, the important natural product and close nicotine analog epibatidine is a potent agonist at $\alpha7$ nAChRs (Table 1). In addition, we have shown that epibatidine participates in the same kinds of interactions with specific residues as nicotine does in receptors at which nicotine is potent (10, 14).

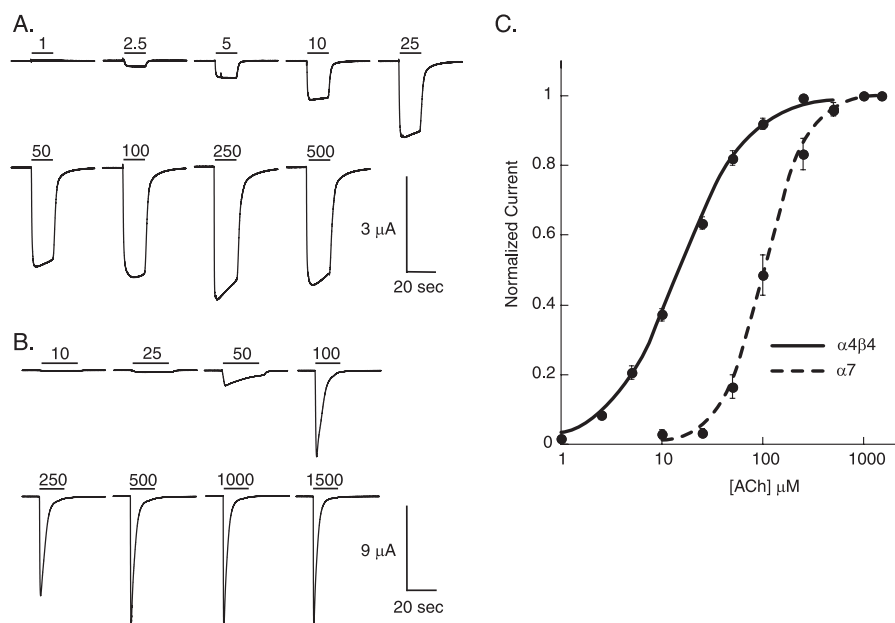FIGURE 3. **Wild type recovery experiments.** *A,* α4β4 nAChR; representative voltage-clamp current traces from oocytes with Trp incorporated by nonsense suppression at position TrpB. *B,* α7 nAChR; representative voltage-clamp current traces from oocytes with Tyr incorporated by nonsense suppression at position TyrC2. In *A* and *B,* bars indicate application of ACh (in μM) at concentrations noted. *C,* dose-response curve and fit of data in *A* and *B* to the Hill equation. The *error bars* indicate S.E. ($n = 10$–13).

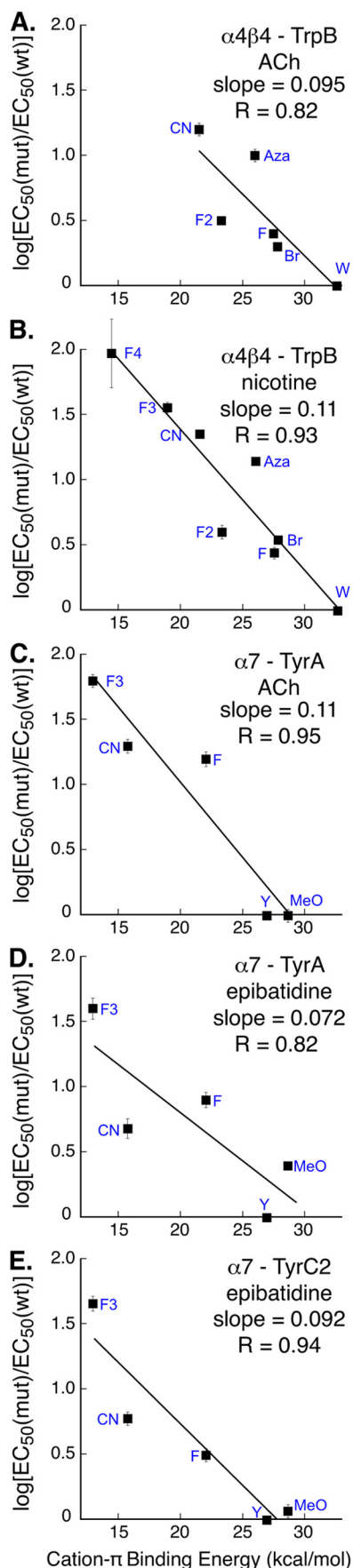As such, our studies of the α7 nAChR have used epibatidine along with ACh.

With the above strategies, unnatural amino acid mutagenesis studies of the α4β4 and α7 receptors proceeded smoothly (Fig. 3). In the present work, we report EC_{50} values, which indicate a functional measure that can be altered by changes in agonist affinity and/or receptor gating. All of our previous studies of the aromatic box of nAChRs have employed this metric, and so using EC_{50} measurements allows direct comparisons between different subtypes. In addition, an earlier study of the α4β2 receptor employed single-channel analysis to establish that shifts in EC_{50} caused by subtle mutations at TrpB, a major focus of the present work, result from changes in agonist affinity, not receptor gating (15).

Ligand Binding Mechanism of the α4β4 Receptor—Our lab has previously established that the muscle-type and α4β2 nAChRs interact with agonists through cation-π interactions at TrpB (12, 15). We therefore focused on TrpB in the α4β4 receptor using strategies that are now well established for identifying a cation-π interaction. In particular, we systematically fluorinate a side chain and determine whether the progressive diminution of the cation-π binding ability of the residue induced by fluorination is manifested in receptor function. The fluorination approach can be augmented with other substitutions, such as the highly deactivating cyano (CN) substituent, which is compared with the much less deactivating but sterically similar bromo substituent. With ACh as the agonist, both the 5-CN-Trp/5-bromo-tryptophan effect (9-fold ratio of EC_{50}; Table 1 and supplemental Table S2) and the fluorination effect (Fig. 4*A*) establish that a cation-π interaction is present at TrpB. Efforts to incorporate 5,6,7-trifluoro-tryptophan or 4,5,6,7-tetra-fluoro-tryptophan gave low expression yields, such that we were unable to achieve large enough signals with ACh as agonist but could do so with nicotine as agonist. To compensate for

the lack of ACh data, we incorporated 7-aza-tryptophan, which is structurally very similar to Trp but shows a diminished cation-π binding ability. When all the data are combined (Trp, 5-fluoro-tryptophan, 5,7-difluoro-tryptophan, 7-aza-tryptophan, 5-bromo-tryptophan, and 5-CN-Trp) into one plot, we observe a linear correlation with *ab initio* calculated cation-π binding energies. The slope of this "fluorination plot" resembles that reported for other nAChRs. A much more thorough study was possible with nicotine as the agonist, producing compelling evidence for a cation-π interaction to TrpB (Fig. 4*B*). Interestingly, when considering the effects of nicotine at TrpB, the cation-π slope resembles that of the α4β2 receptor rather than the muscle-type receptor, which shows no consistent fluorination effect with nicotine as the agonist. Hence, in the α4β4 receptor, similar to the α4β2 receptor (15), nicotine mimics ACh at TrpB with regard to the cation-π interaction.

We performed extensive studies of the remaining components of the aromatic box contributed by the principal face of the ligand-binding domain (TyrA, TyrC1, and TyrC2). Historically, nonsense suppression with tyrosine derivatives has proven more challenging than tryptophan derivatives when one probes for a cation-π interaction. Direct fluorination of tyrosine progressively lowers the pK_a of the side chain hydroxyl group, such that the pK_a for tetrafluorotyrosine is ~5.3 (lowered from ~10 for tyrosine). This decrease in pK_a can lead to ionization of the hydroxyl in unnatural tyrosine analogs. Thus, observed shifts in EC_{50} could result from ionization of the hydroxyl group rather than changes in the cation-π binding ability, complicating analysis. In other receptors, we have circumvented this potential problem by first incorporating phenylalanine, followed by successively fluorinated phenylalanine derivatives, which avoids pK_a complications (46).

In the α4β4 receptor, we found that for TyrA deletion of the hydroxyl group (to give Phe) negatively impacts receptor func-

tion for both ACh and nicotine (Table 1). Interestingly, incorporation of either 4-MeO-Phe or 4-bromo-phenylalanine perturbs receptor function much less, whereas 4-cyano-phenylalanine is strongly perturbing. This represents a distinction in the behavior of TyrA when comparing α4β4 to the α4β2 and muscle-type receptors. For proper receptor function in the α4β4 receptor, it appears that TyrA requires only steric bulk at this position. However, 4-MeO-Phe is highly deleterious in the α4β2 and muscle-type receptors, suggesting that a hydrogen bond donor is required. Successive fluorination of phenylalanine does not result in progressively reduced channel function; we conclude that neither ACh nor nicotine participates in a cation-π interaction with TyrA.

The remaining two residues, TyrC1 and TyrC2, are both contributed by loop C, a very mobile component of the binding site (47). We probed both of these residues for possible hydrogen bonding and cation-π interactions, and we find that TyrC1 and TyrC2 display opposite effects. TyrC1 is highly sensitive to any mutation that obliterates the hydrogen bond donating ability, as evidenced by a rightward shift in EC_{50} of over 50-fold for ACh and 30-fold for nicotine in response to the Phe, 4-MeO-Phe, 4-bromo-phenylalanine, and 4-cyano-phenylalanine mutations (Table 1). This is a phenotype we have seen at TyrC1 for all the nAChRs we have studied, and we interpret it to indicate that the OH of TyrC1 contributes a hydrogen bond that is critical to receptor function. If this position served as a hydrogen bond acceptor, then incorporation of 4-MeO-Phe would have rescued normal channel function. Rather, incorporation of 4-MeO-Phe resulted in substantial loss of channel function; therefore, we conclude that TyrC1 is an important hydrogen bond donor.

In contrast, TyrC2 is quite receptive to mutations of the 4-position hydroxyl group, with many types of substituents accepted and no obvious structure-function relationship. The fact that 4-cyano-phenylalanine gives essentially wild type behavior for both ACh and nicotine would appear to rule out a strong cation-π interaction at this site. These results suggest that TyrC2 participates structurally in shaping the ligand-binding site rather than directly in ligand recognition. Again, the results for both TyrC1 and TyrC2 are similar to what is seen for muscle-type and α4β2.

In α4β4, we also investigated the hydrogen bonding capability of the backbone carbonyl of TrpB (Fig. 1), because this site is known to behave differently in the muscle-type and α4β2 nAChRs (14, 15). By replacing the amino acid at the $i + 1$ position with the analogous α-hydroxy acid, one converts the carbonyl associated with residue i to an ester carbonyl rather than an amide (peptide) carbonyl (Fig. 2C) (14). It is well established that ester carbonyls are poorer hydrogen bond acceptors than amide carbonyls, and so if a hydrogen bond to this carbonyl is essential, the backbone ester mutation should influence agonist potency. With nicotine as the agonist, the backbone ester muta-

FIGURE 4. **Cation-π binding plots, in which log[EC_{50}(mut)/EC_{50}(wt)] is plotted *versus* quantitative cation-π binding energies (12, 35).** The data are from Table 1. Where not visible, the *error bars* are smaller than the data marker. *A* and *B*, cation-π plots for α4β4 nAChR at position TrpB with ACh (*A*) and nicotine (*B*). *C* and *D*, cation-π plots for α7 nAChR at position TyrA with ACh (*C*) and epibatidine (*D*). *E*, position TyrC2 with epibatidine.

tion causes a 14-fold increase in EC_{50} in α4β4 (Table 1). Importantly, the potency of ACh, which cannot make a conventional hydrogen bond to the carbonyl, is essentially unperturbed by the backbone ester mutation. This establishes that the mutation does not globally alter the binding/gating characteristics of the receptor, supporting the notion that we are modulating a hydrogen bonding interaction between the receptor and nicotine. As with TrpB, the behavior of α4β4 is more similar to that of α4β2 rather than muscle-type.

The α7 Receptor Reveals a Different Ligand Binding Mode—Quite surprisingly, in the α7 nAChR, TrpB does not make a cation-π interaction with either ACh or epibatidine as agonist. Incorporation of both 5-CN-Trp and 5,7-difluoro-tryptophan produced functional receptors with essentially wild type behavior (Table 1). Nicotine cannot be systematically studied at the α7 receptor, but we were able to obtain convincing qualitative evidence that EC_{50} is also unperturbed by the 5-CN-Trp mutant with nicotine as the agonist (48).

In other members of the Cys loop family, aromatics other than TrpB make cation-π interactions to their respective agonists. In particular, both TyrA and TyrC2 have been shown to participate in cation-π interactions in select receptors (34, 36). As such, we probed these residues in the α7 receptor.

We noted above that we typically use Phe as a starting point for studies of a Tyr residue to avoid complications associated with the pK_a of the Tyr hydroxyl group. However, Phe is a substantial loss-of-function mutation here. The data suggest that having any substituent at all is preferable to nothing; for example, 4-MeO-Phe is much more nearly wild type. As such, we did not include 3,5-diflouro-phenylalanine, which lacks a substituent in the 4-position, in the cation-π plots.

Considering first TyrA of the α7 receptor, the effect of a 4-substituent is especially pronounced, with the Phe mutant significantly compromised (48-fold for ACh) (Table 1). However, we find that 4-MeO-Phe, 4-bromo-phenylalanine, 4-acetyl-phenylalanine, and, to a lesser extent, 4-methyl-phenylalanine rescued the wild type EC_{50} ([supplemental Table S3](#)). It thus appears that in the α7 nAChR, some substituent is required at the 4-position for proper receptor function. Confirming this observation, when the methoxy or hydroxyl groups are moved to the meta position (3-methoxy-phenylalanine and *meta*-Tyr), receptor function is greatly compromised ([supplemental Table S3](#)). In this regard, the behavior of this TyrA is similar to that observed for the α4β4 receptor, but not the α4β2 or muscle-type receptors, for which the OH appears to be a hydrogen bond donor, not a steric placeholder.

We also gathered data suggesting that in the α7 receptor, TyrA interacts with ACh through a cation-π interaction (Fig. 4C). We can anticipate more scatter in this α7 cation-π plot than is typically seen, because the strong steric effect at the 4-position is overlaid on any electronic effect. For this reason, we have not included especially the bulky bromo substituent. When log(EC_{50}) is plotted *versus* cation-π binding ability for residues designed to probe a cation-π interaction, a clear correlation is seen. Note also that although the fit to the line is not as good as we typically see, the slope is very much in the range of what we observe for cation-π interactions. Thus, we feel the

most reasonable interpretation of the data is that there is a cation-π interaction between ACh and TyrA in the α7 receptor.

In contrast to the results for ACh, when epibatidine is used as agonist, the TyrA plot shows more scatter and a smaller slope (Fig. 4D). It appears that there may be a cation-π interaction present, but if so, it appears to be weaker than normal.

We next considered TyrC2, and, similar to TyrA, the 4-substituent acts as a steric place holder for both ACh and epibatidine. TyrC2 does not interact with ACh through a cation-π interaction (Table 1), as evidenced by the fact that 4-cyano-phenylalanine gives near wild type behavior. However, with epibatidine as the agonist, we observe a clear correlation in the fluorination plot at TyrC2, with a larger slope than seen at TyrA and less scatter (Fig. 4E). We conclude there is a significant cation-π interaction to TyrC2 for epibatidine but not for ACh.

We also explored the functional role of TyrC1 in the α7 receptor. As observed with other nAChRs, this site follows the trend of being highly sensitive to mutation of the 4-position hydroxyl group. Deletion of the hydroxyl group essentially obliterated receptor function as shown by a 90-fold increase in EC_{50}, and incorporation of 4-MeO-Phe, F-Phe, and 3,4,5-tri-flouro-phenylalanine did not yield functional receptors. We also probed other aromatic residues near the aromatic binding box; no compelling effects were observed for these residues ([supplemental Table S3](#)).

We then evaluated the potential hydrogen bond to the backbone carbonyl of TrpB at position Ser-150 in the α7 receptor. For these experiments, we employed the threonine/threonine-α-hydroxy pair, which is the same α-hydroxy acid pair used in α4β4, α4β2, and muscle-type. Table 1 shows that the effect of the Ser-to-Thr mutation is minimal. For α7, the results differ markedly from those observed for α4β4 and α4β2. For epibatidine, the backbone ester substitution minimally raises EC_{50}, but only 2.1-fold (Table 1), whereas for ACh the backbone ester mutation *lowers* EC_{50} ~4-fold. This pattern is very similar to that seen in the muscle-type receptor (14).

DISCUSSION

With >20 nAChR subtypes, these essential neurotransmitter-gated ion channels provide a wide array of targets for pharmaceutical development (1, 2). Given the considerable sequence similarity, especially in the region of the agonist-binding site, it becomes quite challenging to discern the mechanisms for differential activation of homologous receptors. Here, we employ unnatural amino acid mutagenesis to address such questions. This method enables subtle and systematic modifications that can isolate specific binding interactions and provide qualitative guidance on the relative magnitudes of specific interactions.

The primary goal of the present work was to evaluate contributions of the principal binding components of the aromatic box to ligand binding in two neuronal nAChRs: the α4β4 and α7 receptors. Note that the side chains within the aromatic box are identical in all the receptors considered: three tyrosines and two tryptophans. Thus, differences among the receptors must result from subtle structural effects.

Considering the α4β4 receptor, the binding of ACh is similar to what has previously been observed for the muscle-type and

α4β2 receptors. The quaternary ammonium ion of ACh makes a cation-π interaction to the face of the aromatic residue TrpB, providing an unambiguous anchor point for ACh docking. The slopes of the fluorination plots are as follows: 0.095, 0.100, and 0.095 for the α4β4, α4β2, and muscle-type nAChRs, respectively (12, 15). We interpret such similarity in slopes to indicate that the three receptors participate in equally strong cation-π interactions between ACh and TrpB. Further, we find that the roles of the other residues of the aromatic box (TyrA, TyrC1, and TyrC2) are similar to those seen in the muscle-type and α4β2 receptors when binding ACh.

An interesting result is observed when nicotine is the agonist; the neuronal α4β4 receptor acts similarly to the α4β2 receptor rather than to the muscle-type receptor. In α4β4, nicotine makes the same cation-π interaction to TrpB as ACh, consistent with the long-accepted nicotinic pharmacophore, but an interaction that is absent in the muscle-type receptor. Interestingly, the slope of the fluorination plot for α4β4 is 0.11, which could suggest a moderately stronger cation-π interaction at this position than observed for α4β2 (slope = 0.089) (15). Thus, a cation-π interaction to TrpB serves as a discriminator between receptors with higher sensitivity to nicotine (α4β4 and α4β2) and those with lower sensitivity (muscle-type).

Furthermore, α4β4 also behaves like α4β2, not muscle-type, concerning the hydrogen bond to the backbone carbonyl associated with TrpB. At α4β4, nicotine displays a 14-fold decrease in receptor function in response to the backbone ester mutation, comparable with 19-fold for α4β2 and contrasting the value of 1.6-fold for the muscle-type receptor (14, 15). Note that when the agonist is ACh, a molecule unable to make a conventional hydrogen bond to a carbonyl, essentially wild type receptor behavior is observed. This indicates that the backbone mutation did not alter receptor function downstream from binding, *i.e.* gating. We conclude that nicotine is able to make a hydrogen bond to the carbonyl in question in all three receptors considered, but that the interaction is much stronger in the neuronal α4β4 and α4β2 receptors. This is an additional contributor to the enhanced potency of nicotine at the neuronal α4β4 and α4β2 receptors. Previous studies of neuronal nAChRs have indicated that large differences in agonist affinity are primarily determined by the nature of the complementary subunit (49). Our results provide a molecular rationale indicating that both α4-containing neuronal receptors make the same ligand-receptor interactions, but the magnitudes of the two interactions examined differ depending on the receptor, reflecting the nature of the β subunit. The cation-π interaction is stronger in the α4β4 receptor, whereas the hydrogen bond interaction is stronger in the α4β2 nAChR.

We also examined the ligand-binding mechanism of a second neuronal nAChR, the homopentameric α7 receptor. This receptor, an interesting drug target, represents the third α subunit we have probed, and it is novel because the complementary component of the agonist-binding site is also defined by an α subunit. Also, the α7 receptor shows a generically lower affinity than the other neuronal receptors we have considered, and it is interesting to consider whether that behavior is reflected in the aromatic box.

Remarkably, we find that the α7 receptor exhibits a dramatically different binding mode when compared with all of the other nAChRs studied. A strong cation-π interaction to TrpB is seen for ACh at muscle-type, α4β4, and α4β2 and for nicotine at α4β2 and α4β4, but it is completely absent in α7. This result is quite unambiguous; substitution of the native tryptophan with 5-CN-Trp and 5,7-difluoro-tryptophan has no effect on EC_{50} for ACh and the nicotine analog epibatidine. So, despite complete sequence conservation among the five residues that form the aromatic box, ACh adopts two different binding modes in the neuronal nAChRs. To date, every Cys loop receptor we have investigated makes a cation-π interaction (50), so it was not surprising to find one in the α7 receptor. For ACh as agonist, that cation-π site has moved to TyrA. Incorporation of fluorinated phenylalanine derivatives produced a strong, monotonic effect at this site, and although there are steric complications associated with modulating this tyrosine site, the linear correlation of the fluorination plot is good. The large CN/bromo ratio further supports the existence of a cation-π interaction between ACh and TyrA for the α7 receptor.

Interestingly, when examining the effects of epibatidine at TyrA of the α7 receptor (recalling that nicotine is not a viable agonist at α7), the results are more complicated and, to some extent, unprecedented. It is clear that fluorination at TyrA impacts epibatidine potency, and more fluorines have a generally monotonic effect. However, the linear correlation is not as compelling as previously observed in other systems. We interpret the decreased slope for this fluorination plot to indicate a weaker than usual cation-π interaction. It is likely that a weaker cation-π interaction would make the fluorination plot more susceptible to other variations such as steric effects, possibly accounting for the poorer quality of the fit.

When studying epibatidine at TyrC2, a more compelling fluorination plot is obtained, with a better fit and a slope within the normal range of previously reported cation-π interactions. Thus, it appears that epibatidine simultaneously interacts via a cation-π interaction with two residues of the aromatic box: strongly with TyrC2 and moderately with TyrA. Although this marks the first time we have observed such behavior in a Cys loop receptor, it is quite plausible because these two tyrosines are positioned near each other (Fig. 1), and epibatidine is large enough to contact both residues simultaneously. In addition, the protein structural data bank contains many examples of two aromatics making a strong cation-π interaction to a single cation (51). Note that the energetic falloff of the cation-π interaction with distance between the cation and the aromatic is not especially steep (52), and so even a cation that is not in direct van der Waals contact with an aromatic residue experiences a significant stabilization.

The α7 receptor also differs from the other neuronal receptors with regard to the backbone hydrogen bond to the TrpB carbonyl. The strong interaction to the TrpB backbone carbonyl seen in higher affinity receptors (α4β4 and α4β2) is greatly diminished in α7. In fact, with regard to the hydrogen bonding seen with nicotinic-type agonists (but not the cation-π interaction), the α7 receptor is qualitatively similar to the muscle-type receptor. Additionally, both have comparatively low sensitivity for the two ligands tested. Both the muscle-type and
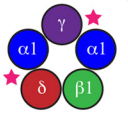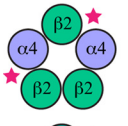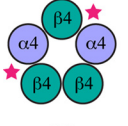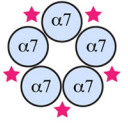
ACh	nicotine epibatidine	
Cation-π	Cation-π	H-bond
TrpB	none TrpB	weak weak
TrpB	TrpB	strong
TrpB	TrpB	strong
TyrA	TyrC2 TyrA	weak

FIGURE 5. **Summary of ligand-receptor interactions present for the muscle-type, α4β2, α4β4, and α7 nAChRs.** *Stars* indicate relevant binding site interfaces.

α7 receptors have a glycine at the position four residues past TrpB, whereas the high affinity α4β4 and α4β2 have a lysine. Modeling studies (53) and mutagenesis studies (15) suggest that this structural change influences the shape of the aromatic box, impacting agonist binding. Note, however, that although α4β4 and α4β2 show generally similar binding behaviors, α7 and muscle-type receptors differ from one another in that ACh binds to TrpB in the muscle-type but to TyrA in α7. As such, other factors must also contribute to the shaping of the agonist-binding site.

We have now studied four members of the nAChR family: muscle-type, α4β2, α4β4, and α7 (Fig. 5). Here we identify structural features of the nAChR that discriminate among these four receptors and are likely to contribute to differential receptor pharmacology. In the muscle-type receptor, TrpB makes a cation-π interaction to ACh and to epibatidine, but not to nicotine (12–14). In the neuronal α4β4 and α4β2 receptors, the TrpB cation-π interaction to ACh remains, but now nicotine also makes a strong cation-π interaction (15). The α7 receptor eschews the cation-π interaction to TrpB, as agonists have moved their cationic center across the aromatic box to TyrA and TyrC2. The nAChR family also uses a backbone hydrogen bonding interaction as a second discriminating feature for drug-receptor interactions. This interaction is modest in the muscle-type and α7 receptors; it is much stronger in α4β4 and α4β2, the higher sensitivity receptors. Taken as a whole, the data support the view that the energy of the cation-π and hydrogen bond interactions studied here underlies the higher sensitivity of these two receptors.

Of course, these observations beg the next question as to what features of the receptor are responsible for these changes, remembering that the residues probed here are conserved in all of the receptors. Further experiments are underway to probe both the non-α subunits and residues within the α subunit that are located outside the aromatic box.

REFERENCES

1. Corringer, P. J., Le Novère, N., and Changeux, J. P. (2000) *Annu. Rev. Pharmacol. Toxicol.* **40,** 431–458
2. Jensen, A. A., Frølund, B., Liljefors, T., and Krogsgaard-Larsen, P. (2005) *J. Med. Chem.* **48,** 4705–4745
3. Romanelli, M. N., Gratteri, P., Guandalini, L., Martini, E., Bonaccini, C., and Gualtieri, F. (2007) *Chem. Med. Chem.* **2,** 746–767
4. Beers, W. H., and Reich, E. (1970) *Nature* **228,** 917–922
5. Glennon, R. A., and Dukat, M. (2000) *Pharm. Acta. Helv.* **74,** 103–114
6. Dart, M. J., Wasicak, J. T., Ryther, K. B., Schrimpf, M. R., Kim, K. H., Anderson, D. J., Sullivan, J. P., and Meyer, M. D. (2000) *Pharm. Acta. Helv.* **74,** 115–123
7. Unwin, N. (2005) *J. Mol. Biol.* **346,** 967–989
8. Brejc, K., van Dijk, W. J., Klaassen, R. V., Schuurmans, M., van Der Oost, J., Smit, A. B., and Sixma, T. K. (2001) *Nature* **411,** 269–276
9. Sixma, T. K., and Smit, A. B. (2003) *Annu Rev Biophys. Biomol. Struct.* **32,** 311–334
10. Blum, A. P., Lester, H. A., and Dougherty, D. A. (2010) *Proc. Natl. Acad. Sci. U.S.A.* **107,** 13206–13211
11. Gotti, C., and Clementi, F. (2004) *Prog. Neurobiol.* **74,** 363–396
12. Zhong, W., Gallivan, J. P., Zhang, Y., Li, L., Lester, H. A., and Dougherty, D. A. (1998) *Proc. Natl. Acad. Sci. U.S.A.* **95,** 12088–12093
13. Beene, D. L., Brandt, G. S., Zhong, W., Zacharias, N. M., Lester, H. A., and Dougherty, D. A. (2002) *Biochemistry* **41,** 10262–10269
14. Cashin, A. L., Petersson, E. J., Lester, H. A., and Dougherty, D. A. (2005) *J. Am. Chem. Soc.* **127,** 350–356
15. Xiu, X., Puskar, N. L., Shanata, J. A., Lester, H. A., and Dougherty, D. A. (2009) *Nature* **458,** 534–537
16. Wu, J., Liu, Q., Yu, K., Hu, J., Kuo, Y. P., Segerberg, M., St John, P. A., and Lukas, R. J. (2006) *J. Physiol.* **576,** 103–118
17. Improgo, M. R., Scofield, M. D., Tapper, A. R., and Gardner, P. D. (2010) *Prog. Neurobiol.* **92,** 212–226
18. Martin, L. F., Kem, W. R., and Freedman, R. (2004) *Psychopharmacology* **174,** 54–64
19. O'Neill, M. J., Murray, T. K., Lakics, V., Visanji, N. P., and Duty, S. (2002) *Curr. Drug Targets CNS Neurol. Disord.* **1,** 399–411
20. Wang, H., Yu, M., Ochani, M., Amella, C. A., Tanovic, M., Susarla, S., Li, J. H., Yang, H., Ulloa, L., Al-Abed, Y., Czura, C. J., and Tracey, K. J. (2003) *Nature* **421,** 384–388
21. Trombino, S., Cesario, A., Margaritora, S., Granone, P., Motta, G., Falugi, C., and Russo, P. (2004) *Cancer Res.* **64,** 135–145
22. Court, J. A., Lloyd, S., Johnson, M., Griffiths, M., Birdsall, N. J., Piggott, M. A., Oakley, A. E., Ince, P. G., Perry, E. K., and Perry, R. H. (1997) *Brain Res. Dev. Brain Res.* **101,** 93–105
23. Zeisel, S. H. (2006) *Annu. Rev. Nutr.* **26,** 229–250
24. Alkondon, M., Pereira, E. F., Cortes, W. S., Maelicke, A., and Albuquerque, E. X. (1997) *Eur. J. Neurosci.* **9,** 2734–2742
25. Vijayaraghavan, S., Pugh, P. C., Zhang, Z. W., Rathouz, M. M., and Berg, D. K. (1992) *Neuron* **8,** 353–362
26. Arneric, S. P., and Brioni, J. D. (1999) *Neuronal Nicotinic Receptors: Pharmacology and Therapeutic Opportunities*, Wiley-Liss, Inc., New York
27. Orr-Urtreger, A., Göldner, F. M., Saeki, M., Lorenzo, I., Goldberg, L., De Biasi, M., Dani, J. A., Patrick, J. W., and Beaudet, A. L. (1997) *J. Neurosci.* **17,** 9165–9171
28. Stevens, K. E., Freedman, R., Collins, A. C., Hall, M., Leonard, S., Marks, M. J., and Rose, G. M. (1996) *Neuropsychopharmacology* **15,** 152–162
29. Stevens, K. E., Kem, W. R., Mahnir, V. M., and Freedman, R. (1998) *Psychopharmacology* **136,** 320–327
30. Séguéla, P., Wadiche, J., Dineley-Miller, K., Dani, J. A., and Patrick, J. W. (1993) *J. Neurosci.* **13,** 596–604
31. Zhang, Z. W., Vijayaraghavan, S., and Berg, D. K. (1994) *Neuron* **12,** 167–177
32. Saks, M. E., Sampson, J. R., Nowak, M. W., Kearney, P. C., Du, F., Abelson, J. N., Lester, H. A., and Dougherty, D. A. (1996) *J. Biol. Chem.* **271,** 23169–23175
33. Nowak, M. W., Gallivan, J. P., Silverman, S. K., Labarca, C. G., Dougherty, D. A., and Lester, H. A. (1998) *Methods Enzymol.* **293,** 504–529

34. Padgett, C. L., Hanek, A. P., Lester, H. A., Dougherty, D. A., and Lummis, S. C. (2007) *J. Neurosci.* **27,** 886–892

35. Lummis, S. C., Beene, D., Harrison, N. J., Lester, H. A., and Dougherty, D. A. (2005) *Chem. Biol.* **12,** 993–997

36. Mu, T. W., Lester, H. A., and Dougherty, D. A. (2003) *J. Am. Chem. Soc.* **125,** 6850–6851

37. Torrice, M. M., Bower, K. S., Lester, H. A., and Dougherty, D. A. (2009) *Proc. Natl. Acad. Sci. U.S.A.* **106,** 11919–11924

38. Moroni, M., Zwart, R., Sher, E., Cassels, B. K., and Bermudez, I. (2006) *Mol. Pharmacol.* **70,** 755–768

39. Nelson, M. E., Kuryatov, A., Choi, C. H., Zhou, Y., and Lindstrom, J. (2003) *Mol. Pharmacol.* **63,** 332–341

40. Halevi, S., McKay, J., Palfreyman, M., Yassin, L., Eshel, M., Jorgensen, E., and Treinin, M. (2002) *EMBO J.* **21,** 1012–1020

41. Ben-Ami, H. C., Yassin, L., Farah, H., Michaeli, A., Eshel, M., and Treinin, M. (2005) *J. Biol. Chem.* **280,** 28053–28060

42. Castillo, M., Mulet, J., Gutiérrez, L. M., Ortiz, J. A., Castelán, F., Gerber, S., Sala, S., Sala, F., and Criado, M. (2005) *J. Biol. Chem.* **280,** 27062–27068

43. Cheng, A., McDonald, N. A., and Connolly, C. N. (2005) *J. Biol. Chem.* **280,** 22502–22507

44. Williams, M. E., Burton, B., Urrutia, A., Shcherbatko, A., Chavez-Noriega, L. E., Cohen, C. J., and Aiyar, J. (2005) *J. Biol. Chem.* **280,** 1257–1263

45. Placzek, A. N., Grassi, F., Meyer, E. M., and Papke, R. L. (2005) *Mol. Pharmacol.* **68,** 1863–1876

46. Nowak, M. W., Kearney, P. C., Sampson, J. R., Saks, M. E., Labarca, C. G., Silverman, S. K., Zhong, W., Thorson, J., Abelson, J. N., Davidson, N., Schultz, P. G., Dougherty, D. A., and Lester, H. A. (1995) *Science* **268,** 439–442

47. Espinoza-Fonseca, L. M., and Trujillo-Ferrara, J. G. (2006) *Bioorg. Med. Chem. Lett.* **16,** 3519–3523

48. Xiu, X. (2007) *Structure-Function Studies of Nicotinic Acetylcholine Receptors Using Unnatural Amino Acids*, pp. 67–100, California Institute of Technology, Pasadena, CA

49. Parker, M. J., Beck, A., and Luetje, C. W. (1998) *Mol. Pharmacol.* **54,** 1132–1139

50. Dougherty, D. A. (2008) *Chem. Rev.* **108,** 1642–1653

51. Gallivan, J. P., and Dougherty, D. A. (1999) *Proc. Natl. Acad. Sci. U.S.A.* **96,** 9459–9464

52. Dougherty, D. A. (1996) *Science* **271,** 163–168

53. Grutter, T., Prado de Carvalho, L., Le Novère, N., Corringer, P. J., Edelstein, S., and Changeux, J. P. (2003) *EMBO J.* **22,** 1990–2003